Research Journal of Applied Sciences, Engineering and Technology 7(14): 2868-2873, 2014
DOI:10.19026/rjaset.7.612
ISSN: 2040-7459; e-ISSN: 2040-7467

Submitted: February 06, 2013 Accepted: March 02, 2013 Published: April 12, 2014

Research Article

Performance Test and Evaluation for Pixel CdZnTe Detector of Different Thickness

[1, 3]Shen Min, [1]Xiao Shali, [1]Zhang Liuqiang, [2]Cao Yulin and [2]Chen Yuxiao
[1]Key Lab of Optoelectronic Technology and Systems, Ministry of Education,
Chongqing University, China
[2]Institute of Electronic Engineering, China Academy of Engineering Physics, Si Chuan, China
[3]ChongQing Technology and Business Institute, ChongQing, China

Abstract: The aim of this study is to get the photon energy suitable for different thickness detector, different photon energy acts on pixel CdZnTe detector of different thickness. We can obtain the energy spectrum estimation, energy resolution and peak efficiency by the experiment and simulation with the radiation source of 241Am and 137Cs acting on pixel CdZnTe detector. From experiment results, it can be found that at the high energy of 662 keV the thicker the CdZnTe detector is, the higher the energy resolution and peak efficiency is while at the low energy of 59.5 keV tailing increases and charge is loss. It also can be found the characteristic of detector is better at the low energy when the detector thickness is thinner.

Keywords: CdZnTe detector, energy resolution, light spectrum, peak efficiency

INTRODUCTION

In recent years, with the innovation of crystal growth technology and equipment manufacturing technology, the interest for the room temperature semiconductor of high atomic number Z is rising (Li *et al*., 2005; Zha *et al*., 2008; Washington II *et al*., 2010). In these semiconductor materials, CdZnTe material is considered to be suitable for making X-ray and gamma-ray detector. With a high atomic number (Zmax = 52), high-density (ρ = 5.76 g □ cm^3 of) and a wide band gap (Eg~1.6eV) and therefore CdZnTe detector has a high quantum efficiency, good room-temperature characteristics and high stopping power for X-ray and the gamma-ray. Based on these advantages, it is feasible to use CdZnTe detector at the situations of multispectral and low-flow (Szeles, 2004; Sordo *et al*., 2009). In fact, CdZnTe detectors have potential application in high energy situations such as SG-III prototype laser device and synchrotron radiation. Due to the different transmission characteristics of the electron and hole, the performance of the detector is determined primarily by the particle of drift poor life. For CdZnTe material, the biggest flaw is the bad transmission characteristics of the hole. This feature also limits the thickness of the detector, thus the energy range for using the detectors is greatly reducing.

To overcome the transmission characteristics of the holes, researchers have developed charge carrier's detector only collected electronic, such as Frisch gate (Bolotnikov *et al*., 2006a), coplanar gate (Prettymana *et al*., 2002), micro-strip (Montémont *et al*., 2006) and the pixel (Guerra *et al*., 2009) structure detectors. In these single electrode structure, the pixel structure is considered to be best improve the induced charge generated by electron movement to the anode and can reduce the influence of the hole to the minimum (Wangerin *et al*., 2011). At ambient conditions, the pixel CdZnTe detectors exhibit a good energy and spatial resolution. In addition, with surveys and studies it can be found that spectral characteristics of the detected signal can be improved by optimize the geometry of the detector, so that the pixel detectors can achieve maximum efficiency and energy resolution (Aillon *et al*., 2006; Kim *et al*., 2011). Some researchers have constructed electron transport and induced current models of CdZnTe semiconductor detectors (Benoit and Hamel, 2009; Kozorezov and Wigmorea, 2005). However, for the whole equipment, the influence of the hole cannot completely eliminate. Furthermore, since electron trapping caused by the detector impurities and structural defects, the total induced current depends on the distance of pulse height spectrum with a significant trapping trailing. And the spectrum is generated during the particle transfer.

The objective of the study is to get the photon energy suitable for different thickness detector, different photon energy acts on pixel CdZnTe detector of different thickness by the experiment and simulation using the radiation source of 241Am and 137Cs acting on pixel CdZnTe detector.

Corresponding Author: Shen Min, Key Lab of Optoelectronic Technology and Systems, Ministry of Education, Chongqing University, China

METHODOLOGY

In order to study the response of CdZnTe detectors, Monte Carlo was employed to simulate 241Am and 137Cs spectrum. The simulation result was compared with the data obtained by the radioactive source experiments. The comparison results used to assess characteristic parameters such as energy resolution and peak resolution to find compromise detector thickness at different size detectors in the energy of 59.5 and 662 keV. This thickness is suitable for pinhole and a half hole imaging at Inertial Confinement Fusion (ICF).

Pixel CdZnTe detectors of different thickness was tested in the experiment. The detector used in the test is made from CdZnTe single crystal grown from accelerated crucible rotation technique Bridgman (Tao *et al*., 2009). Each surface of the detector size is 10×10 mm. And the thickness is 1, 2, 3 and 5 mm, respectively. The anode surface composed of the 16 pixels arranged in a 4×4 array. A guard ring was employed around the pixel array for reducing the leakage current and the influence of the edge effect. Each pixel in the array is embedded in a recess of 2.38 mm in the vertical and horizontal directions: 1.52 mm for the size of the pixels, 0.86 for the dimensions of the channel. The cathode covers the planar electrode of the entire detector surface. The surfaces of the anode and the cathode are by gold sputtering. The detector pixel anode by reserving the test hole and mat printed circuit board glued together. When the pixel length L is much larger than the pixel size A, the small pixel effect will play a role (Guerra *et al*., 2009). Experiments, the ratio of the pixel pitch W, to the pixel length L can precisely reflect the detector spatial resolution. Therefore, W/L can be considered with 2.380, 1.190, 0.793 and 0.476, respectively. Two sources of 241Am and 137Cs are used to correct. Table 1 summarizes the relevant data for these sources. Radioactive sources employed guide plate of 15 mm for thick Focus. The guide plate has a diameter of 3.2 mm at its center pinhole. Therefore, the gamma rays column just can radiate to each CdZnTe detector pixels.

In the X-ray and gamma-ray semiconductor detectors, the electric field distribution greatly affects the charge collection properties. Trapping effect is related to the high mean electric field. Trapping effect affects the mean free drift distance λ of the carrier to limit the collection efficiency of the charge. $\lambda = v\tau = \mu E\tau$, Where μ represents the mobility of the carrier; v is the drift velocity and E represents a density of electric field; τ is the free drift time. The strength of the electric field in the detector is the manifestation for a certain level of the drift velocity. And there is not much dependence with the applied bias (Bolotnikova *et al*., 2003). But improving the bias means the introduction of more surface leakage current. The leakage current can cause degradation of the energy resolution and peak efficiency. Therefore, bias should be the role of the compromise of the two boycotts. i.e., improve the bias can increase the collection efficiency of the charge.

Table 1: Data for CdZnTe detector experimental radiation source

Sources	Half-life	Energy (keV)	Emission probabilities (%)
^{241}Am	432.7±0.4 (years)	3.300	0.0640
		11.900	0.0860
		13.900	0.1350
		17.800	0.2100
		20.800	0.0500
		26.400	0.0250
		59.500	0.3590
^{137}Cs	11,009±11 (days)	36.400	0.0139
		31.817	0.0207
		32.194	0.0382
		662	0.8998

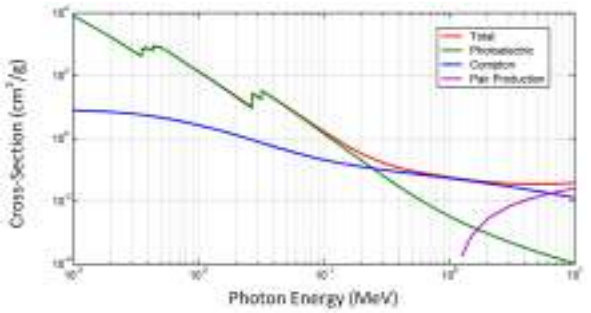

Fig. 1: Cd0.9Zn0.1Te internal interactions

And due to the increase in the leakage current at the same time more noise will be introduced. In addition, in order to exclude the influence of the different electric field strength, electric field strength keeps 130 V/mm constants. This means that, the cathode bias of the detector of -130, -260, -390 and -650 volts for 1, 2, 3 and 5 mm thick, respectively.

Emitter for simulation gamma data is described in Table 1. Simulation energy of the gamma ray can be low to 10 keV. Because gamma column through the collimator radiated to only one pixel of each detector, detector model built using the Monte Carlo method, due to the small pixel effect, can be viewed as a single anode detector. CdZnTe sectional data are obtained from NIST database. The interest of cross-sectional study is the role of the optical field, Compton scattering and produce. Rayleigh scattering is only to change the direction of the energy (Hossain *et al*., 2008; Bolotnikov *et al*., 2006b) without causing any loss of energy. So it may not be considered in the simulation. CdZnTe-section is shown in Fig. 1. CdZnTe-section figure shows in the 0.3 MeV photoelectric effect and Compton scattering at the cross-section are interactions and in the 0.7 MeV the Compton scattering is interaction at the cross-section.

The induced charge in the anode can be calculated with two right weighting factors (charge) of Ramo-Shockley theory (He, 2001). Using this method, the charge Q anode caused by the N independent electron carrier in the anode is related with the end position (xe, ye, ze) and (Xh, Yh, Zh) for each of electrons and holes (He, 2001):

$$Q_{anode} = \sum\nolimits_{N} \Phi_{anode}(x_e, y_e, z_e) - \Phi_{anode}(x_h, y_h, z_h) \quad (1)$$

where in, Φ anode is the charge of the anode weight. In our simulation, a gamma photons at different points (xi, yi, zi) occurs several interactions with CdZnTe material. This series of impacts produced a series of Compton Effect. And it may be eventually absorbed by the photoelectric field. In each point of action, energy ENi generated accumulation. The induced charge Qi in the anode is caused by Ni electron carriers randomly generated by every the energy accumulation to drift to the electrodes. The model contains the sum of the induced charge in the i-th carrier. The charge accumulation and polarization effects have little impact on the experiment at the low photon flux. So it will be ignored in the simulation.

In the experimental spectrum, data symmetrical with energy line was a Gaussian-like distribution. Therefore, more results were obtained through simulation. These results should be considered using a Gaussian function for spectral analysis. In the calculation, the adjusted nonlinear function of least square method was used to calculate the coefficients "a", "b" and "c" point. This coefficient will serve as the input of the Monte Carlo code. The fit function is shown in Eq. (2):

$$FWHM = a + b\sqrt{E + cE^2} \tag{2}$$

where, E stands for the use of gamma-ray energy (MeV); a, b and c stand for the fit function constants of the user. If the energy accumulation are between E0-2.96σ and E0+2.96σ, wherein σ = FWHM/2.35, then it can be considered as the peak at the energy E0. This criterion Integrates 99.7% peak area. For the whole region, light peak efficiency can be obtained with the peak count divided by the number of photons emitted energy.

RESULTS

Version 1.30 of Monte Carlo MCNP5 code was employed to calculate the number of particles produced in the whole process. The run number of particle for every time should be large enough to achieve more satisfactory uncertainty. In the MCNP5 manual, this rule makes the relative uncertainty less than 10%. Nevertheless, at outset of the 107 source particles, the Monte Carlo simulation allows running enough time to get a large number of particles to ensure the statistical uncertainty of less than 1%. For 241Am source, photon energy increases from 10 to 70 keV at the increment of 0.5 keV, while for 137Cs source, the photon energy increases from 10 to 700 keV at the increment of 1 keV. In MCNP5, particles transmission takes multi-channel processor simulation.

Figure 2 and 3 shows a comparison between the experimental data and simulation data. Pulse height distribution obtained by calculating the maximum count of the light at the peak-to-peak meets with normalized

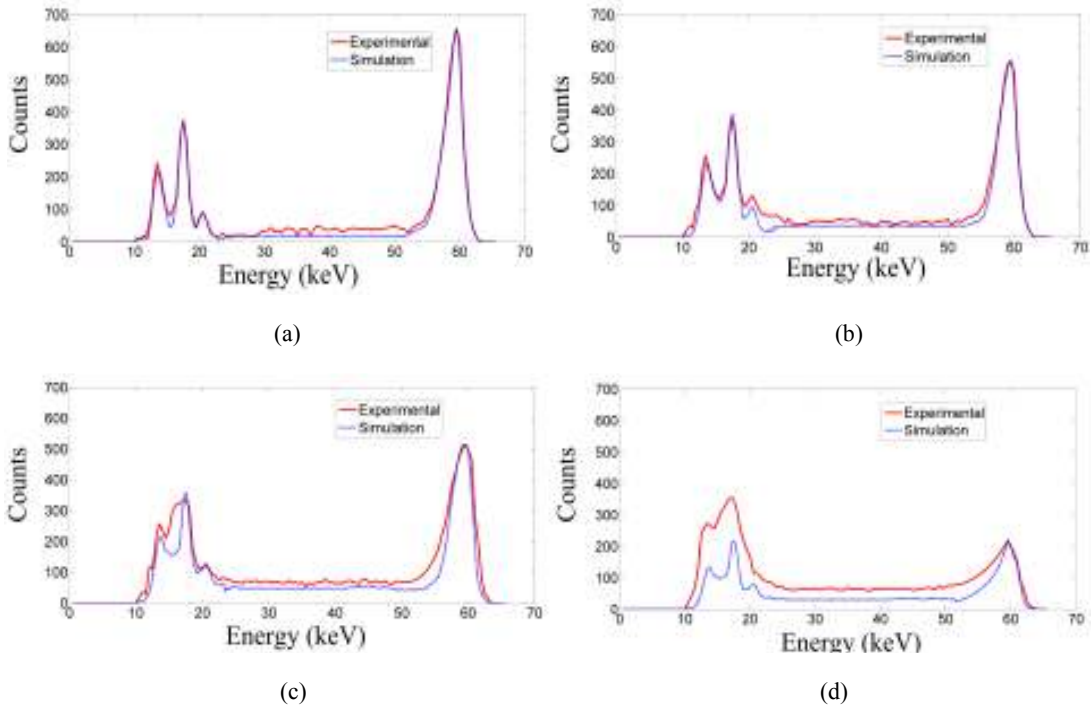

Fig. 2: Comparison between different thickness of the detector pulse height distribution of the experimental data and simulation data under 241Am radiation source, (a) 1 mm, (b) 2 mm, (c) 3 mm, (d) 5 mm

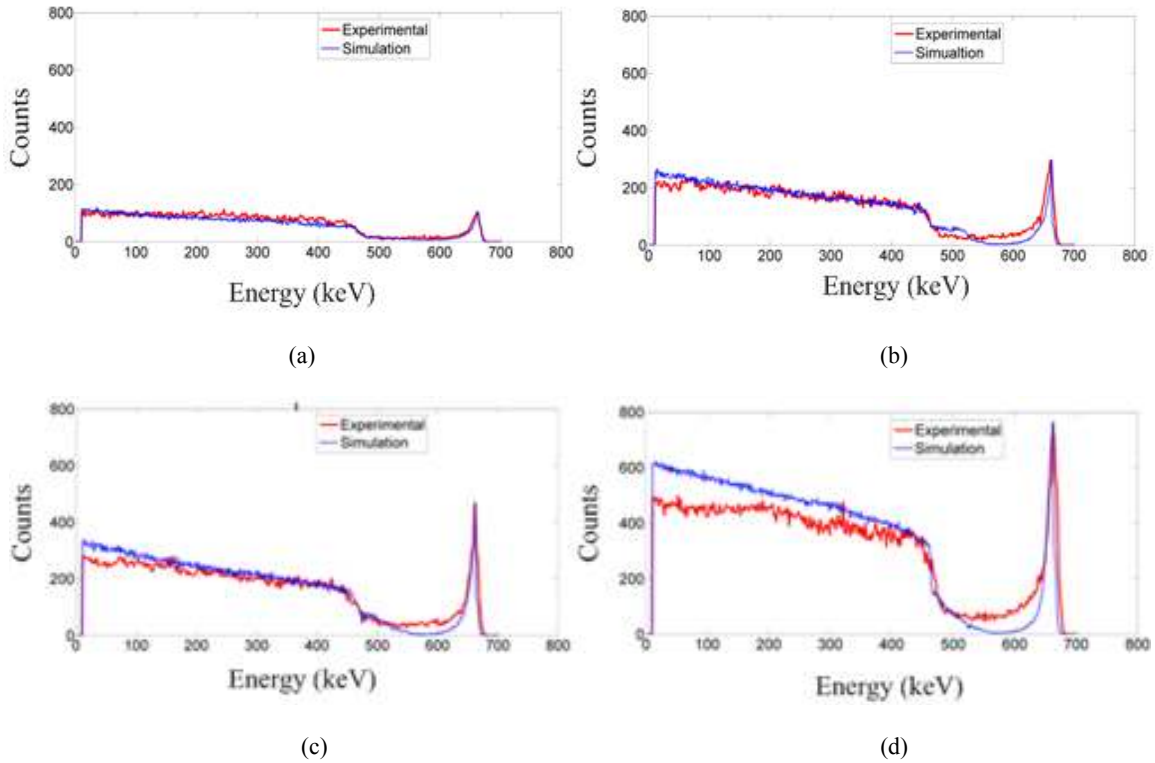

Fig. 3: The energy spectrum of the different detectors under ^{137}Cs radiation source. The figure also shows the experimental data and simulation data. Thickness, respectively: (a) 1 mm, (b) 2 mm, (c) 3 mm and (d) 5 mm

Table 2: The light peak efficiency of different thickness of CdZnTe detector: experimental data and simulation data

		CdZnTe thickness			
		1 mm (%)	2 mm (%)	3 mm (%)	5 mm (%)
^{241}Am	Simulation	47.72	39.83	37.02	29.89
	Experiment	43.53	36.97	35.19	23.94
^{137}Cs	Simulation	0.84	1.50	2.60	5.25
	Experiment	1.07	2.87	4.10	6.58

Table 3: Resolution for CdZnTe detector of different thickness

		CdZnTe thickness			
		1 mm (keV)	2 mm (keV)	3 mm (keV)	5 mm (keV)
^{241}Am	Simulation	2.98	3.33	3.76	3.78
	Experiment	3.03	3.56	4.61	4.82
^{137}Cs	Simulation	13.52	15.74	15.91	16.13
	Experiment	16.90	16.77	16.54	16.52

law. Figure 2 emphasizes the results of the simulation pulse distribution for every time. Stacking and detection efficiency of the mentioned part energy in the above-described Eq. (3) are considered in Fig. 3. This can be drawn that the light peak experimental results are unified for 241Am and 137Cs radiation source.

Figure 2 shows the results of CdZnTe detectors of different thickness for the 241Am radiation source at the energy of 59.5 keV under gamma-ray. Meanwhile, Fig. 3 shows the results obtained for the 137Cs radiation sources at the energy of 662 keV. The peaks of these spectra are consistent with the excitation energy (59.5 or 662 keV). However, their tail is the result of Compton scattering and detection efficiency depending on the depth of role together. The peak efficiencies of the light detector obtained by experiment and simulation of different thicknesses are shown in Table 2 and 3 summarizes the energy resolution.

Figure 2 show the increase in the thickness of the detector will weaken its peak efficiency in the energy resolution and optical characteristics. Because of the low-energy tail, there is crest asymmetric shape in 59.5 keV. Due to the change in the waveform caused by the low energy tailing, FWHM distribution becomes broader in energy of 59.5 keV. Due to the lower energy, the photons of radiation source ^{241}Am only penetrate a

short distance into the crystal. The total electron loss and trapping is proportional to the distance of the electron cloud transmission. The even worse situation is that the low collection efficiency of the electron makes some electronics uncollected by the anode pixel electrodes, which results in loss of signal. These phenomena are not detected in the experiment, further reducing the detection efficiency and the light peak efficiency. But this can be obviously seen from the diagrams of the light peak efficiency and energy resolution for the detector at the thickness of 1 and 5 mm. Therefore, it can be drawn from these results that there will be more electrons loss and trapping for the thickness detector.

As can be seen from Fig. 3, compared to the thick detectors, the thin detector characteristics is limited by the absorption efficiency of photon. Increase the detector thickness will have better energy characteristics for photon absorption efficiency and light peak efficiency. In fact, in the high-energy portion, the Compton scattering plays a major role. Thick detector will have greater sensitivity. In the low energy range, increasing the thickness of the CdZnTe crystals can improve the Compton continuum. This point can be seen from the spectral that increases of the thickness of the detector. It is no improvement in the amount of resolution. In fact, the energy resolution of the change is very small for the thickness varied from 1 to 5 mm, respectively.

DISCUSSION

For ^{37}Cs source, high-energy photons can penetrate the entire crystal (thick ≤5 mm). The role incident of photons occurs near the anode which has poor shielding effect. From Fig. 3 the low energy tailing can be seen from the pulse height spectrum. And it is relevant with photon role events occurred near the anode. The experiments prove that thick detector of the small volume has slightly higher energy resolution and light peak efficiency in the low energy. While for the high energy, the thickness detectors of large volume have better characteristics. At the low energy, the majority of gamma rays act on the vicinity of the cathode. And increasing the thickness of the detector will cause more electronic lost and incomplete collection of electronic. Thereby, the energy resolution and the light peak efficiency are reduced. On the contrary, Compton scattering plays a major role in the high-energy. Therefore, increasing the thickness of the detector can improve its sensitivity, thereby improving the light peak efficiency. Although the increase the detector thickness in the low-energy range can improve the Compton continuum, the improved detection efficiency makes the energy resolution t change insignificantly. This thanks to the small pixel effect caused by the increase in the thickness and decrease of W/L ratio. Five millimeter of the detector and W/L ratio of 0.476 (<0.5) can cause a small pixel effect which prevents the loss of the electron carrier. Thus, in our experiments, the dominant effect is the loss of the electron cloud.

In addition, these data show that compared with the experimental results, the simulation results have usually better energy resolution. But the light peak efficiency of simulation data is low. The possible reason for such a situation is that the calculation of peak efficiency depends on the energy resolution (FHWH). The difference between the experimental values and simulation values can be attributed to the imperfect complex geometry of detectors or internal defects of the detector. And it is also related with incomplete electron collection process. It is known that the Monte Carlo code can obtain data compared with the experimental procedure even the most simple example. Taking into account the current work, the results were amended. Because there is no accumulation of experience, the differences between the calculated and measured values can be accepted.

In ICF, the sensitivity is as high as possible in the high-energy case for pinhole or penumbral imaging system for diagnosis explosive target. The high-energy peak efficiency in the energy of Compton edge has fluctuations. In the low-energy cases, the thin detector can easily obtain a high efficiency. Therefore, energy resolution can be optimized to obtain reasonable detection efficiency. On the other hand, for high energy, the light peak efficiency is the main consideration within the acceptable range of the resolution. All these combined data show that thickness of pixel CdZnTe detector is approximately 1 mm in the low energy of 59.5 keV and the thickness is 5 mm in the high energy of 662 keV.

With different gamma-energy photons, energy spectrum and the theoretical values of light peak efficiency for different thickness CdZnTe detector have a high degree of consistency with experimental values. Increase the thickness of the CdZnTe crystals will exacerbate the loss of CdZnTe internal electronic. Because in the thick crystal, the electron will be transmitted over longer distances and cause more trapped. Therefore, the thickness of the crystal should be thinner as well for similar to the radiation source of ^{241}Am at the low energy of 59.5 keV. At the same time, a thin CdZnTe crystal has low photon attenuation characteristics under the radiation sources of ^{137}Cs at the energy of 662 keV. Therefore, the thickness of the CdZnTe crystals must be large enough to provide more high-energy photon accumulation. Meanwhile, the thickness of the CdZnTe crystal must be large enough to get better detector efficiency.

CONCLUSION

From the above discussion, the following conclusions can be obtained:

- In our experiments, the dominant effect is the loss of the electron cloud.
- The differences between the calculated and measured values can be accepted.
- Energy resolution can be optimized to obtain reasonable detection efficiency. On the other hand, for high energy, the light peak efficiency is the main consideration within the acceptable range of the resolution.
- With different gamma-energy photons, energy spectrum and the theoretical values of light peak efficiency for different thickness CdZnTe detector have a high degree of consistency with experimental values.

ACKNOWLEDGMENT

Our research work has been supported by the Natural Science Foundation of China. And the Fund No. is 0.10876044. This is also the central university basic research fund project, Project No.: CDJXS11122219.

REFERENCES

Aillon, E.G., J. Tabary, A. Gliere and L. Verger, 2006. Charge sharing on monolithic CdZnTe gamma-ray detectors: A simulation study. Nucl. Instrum. Meth. A, 563: 124-127.

Benoit, M. and L.A. Hamel, 2009. Simulation of charge collection processes in semiconductor CdZnTe γ-ray detectors. Nucl. Instrum. Meth. A, 606(3): 508-516.

Bolotnikov, A.E., G.C. Camarda, G.A. Carini, M. Fiederle, L. Li, D.S. McGregor, W. McNeil, G.W. Wright and R.B. James, 2006a. Performance characteristics of Frisch-ring CdZnTe detectors. IEEE T. Nucl. Sci., 53(2): 607-614.

Bolotnikov, A.E., G.S. Camarda, G.A. Carini, Y. Cui, K.T. Kohman, L. Li, M.B. Salomon and R.B. James, 2006b. Performance-limiting defects in CdZnTe detectors. IEEE T. Nucl. Sci., 54(4): 821-827.

Bolotnikova, A.E., C.M. Hubert Chena, W.R. Cooka, F.A. Harrisona, I. Kuvvetlib, S.M. Schindlera, C.M. Stahlec and B.H. Parker, 2003. The effect of cathode bias (field effect) on the surface leakage current of CdZnTe detectors. Nucl. Instrum. Meth. A, 510(3): 300-308.

Guerra, P., A. Santos and D.G. Darambara, 2009. An investigation of performance characteristics of a pixellated room-temperature semiconductor detector for medical imaging. J. Phys. D Appl. Phys., 42(17): 11.

He, Z., 2001. Review of the Shockley-Ramo theorem and its application in semiconductor gamma-ray detectors. Nucl. Instrum. Meth. A, 436(1): 250-267.

Hossain, A., A.E. Bolotnikov, G.S. Camarda, Y. Cui, G. Yang and R.B. James, 2008. Defects in cadmium zinc telluride crystals revealed by etch-pit distributions. J. Cryst. Growth., 310(21): 4493-4498.

Kim, J.C., S.E. Anderson, W. Kaye, F. Zhang, Y. Zhu, S.J. Kaye, Z. He, 2011. Charge sharing in common-grid pixelated CdZnTe detectors. Nucl. Instrum. Meth. A, 654(1): 233-243.

Kozorezov, A.G. and J.K. Wigmorea, 2005. Analytic model for the spatial and spectral resolution of pixellated semiconducting detectors of high-energy photons. J. Appl. Phys., 97(7): 4502-074502.

Li, G., X. Zhang, H. Hua and W. Jie, 2005. A modified vertical Bridgman method for growth of high-quality Cd1-xZnxTe crystals. J. Electron. Mater., 34(9): 1215-1224.

Montémont, G., M.C. Gentet, O. Monnet, J. Rustique and L. Verger, 2006. Simulation and design of orthogonal capacitive strip CdZnTe detectors. IEEE T. Nucl. Sci., 54(4): 3762-3766.

Prettymana, T.H., K.D. Ianakieva, S.A. Soldnerb and C. Szelesb, 2002. Effect of differential bias on the transport of electrons in coplanar grid CdZnTe detectors. Nucl. Instrum. Meth. A, 476: 658-664.

Sordo, S.D., L. Abbene, E. Caroli, A.M. Mancini, A. Zappettini and P. Ubertini, 2009. Progress in the development of CdTe and CdZnTe semiconductor radiation detectors for astrophysical and medical applications. Sensors, 9(5): 3491-3526.

Szeles, C., 2004. CdZnTe and CdTe materials for X-ray and gamma ray radiation detector applications. Phys. Status Solidi. B, 241(3): 783-790.

Tao, W., J. Wan-qi, X. Ya-Dong, Z. Gang-Qiang and F. Li, 2009. Characterization of CdZnTe crystal grown by bottom-seeded Bridgman and Bridgman accelerated crucible rotation techniques. T. Nonferr. Metal. Soc., 19: s622-s625.

Wangerin, K., Y. Du and F. Jansen, 2011. CZT performance for different anode pixel geometries and data corrections. Nucl. Instrum. Meth. A, 648(1): S37-S41.

Washington II, A.L., L.C. Teague, M.C. Duff, A. Burger, M. Groza and V. Buliga, 2010. Atmospheric effects on the performance of CdZnTe single-crystal detectors. J. Electron. Mater., 39(7): 1104-1109.

Zha, M., A. Zappettini, D. Calestani, L. Marchini, L. Zanotti and C. Paorici, 2008. Full encapsulated CdZnTe crystals by the vertical Bridgman method. J. Cryst. Growth., 310(7-9): 2072-2075.